**Separation Science and Technology**
Publication details, including instructions for authors and subscription information:
http://www.informaworld.com/smpp/title~content=t713708471

# ADSORPTION AND DESORPTION OF PHENOL ON ACTIVATED CARBON FIBERS IN A FIXED BED

Ping Li[a]; Guo-Hua Xiu[b]; Lei Jiang[b]
[a] Department of Chemical Engineering, Shenyang Institute of Chemical Technology, Shenyang, P. R. China [b] Center of Molecular Science, Institute of Chemistry, Chinese Academy of Sciences, Beijing, P. R. China

**To cite this Article** Li, Ping , Xiu, Guo-Hua and Jiang, Lei(2001) 'ADSORPTION AND DESORPTION OF PHENOL ON ACTIVATED CARBON FIBERS IN A FIXED BED', Separation Science and Technology, 36: 10, 2147 — 2163
**To link to this Article: DOI:** 10.1081/SS-100105910
**URL:** http://dx.doi.org/10.1081/SS-100105910

SEPARATION SCIENCE AND TECHNOLOGY, 36(10), 2147–2163 (2001)

# ADSORPTION AND DESORPTION OF PHENOL ON ACTIVATED CARBON FIBERS IN A FIXED BED

**Ping Li,[1] Guo-Hua Xiu,[2,*] and Lei Jiang[2]**

[1]Department of Chemical Engineering,
Shenyang Institute of Chemical Technology,
Shenyang, 110021, P. R. China
[2]Center of Molecular Science,
Institute of Chemistry, Chinese Academy of Sciences,
P. O. Box 2709, Beijing, 100080, P. R. China

## ABSTRACT

The application of activated carbon fibers (ACFs) to remove phenol from water is studied. The adsorption capacity of ACFs is favorable and the adsorption isothermal data can be represented by Langmuir-type equation for phenol concentrations changed from 0 to 0.8 kg/m$^3$. The regeneration of ACF adsorbent saturated with phenol in a fixed bed can be achieved by using ethanol or sodium hydroxide solution, respectively, many times with 90% efficiency of regeneration. A mathematical model is applied to evaluate the effects of intraparticle and external mass transfer resistances as well as the axial dispersion on the breakthrough curves. The axial dispersion is confirmed to be the main parameter that controls the adsorption kinetics.

---

*Corresponding author. E-mail: ghxiu@hotmail.com

*Key Words*: Activated carbon fiber; Adsorption; Desorption; Phenol; Fixed-bed; Mathematical model

## INTRODUCTION

Phenolic compounds are pollutants of priority concern that enter the aquatic environment through direct discharge from industries such as coke ovens in steel plants, oil refineries, phenolic resin plants, pharmaceutical and pesticide manufacturers, and so on. Attention has been given to the removal of phenolic compounds from the industrial wastewater by many researchers in the world, for example, removal of phenolic compounds by adsorption (1,2), by microbial degradation (3), by peroxidase-catalyzed oxidation (4,5) and so on. Of these, adsorption is an effective technique for the removal of phenol from water to a lower level for our industries. Many theoretical and experimental works have been published on this subject where adsorbents are activated carbon (6–8), clay (9), and polymeric resins (10,11).

Activated carbon fibers (ACFs) are a new type of high-efficiency adsorbents. Their adsorption capacity is favorable, and higher mass transfer rates for both adsorption and desorption can be obtained, compared with granular and powdered adsorbents, due to their thin fiber shape. In addition, the fibrous form is also favored because of ease in handling when it is used in felt or fabric forms and of availability in consolidated forms by newly developed molding techniques. Also, ACFs have received increasing attention in recent years as adsorbents for purifying air and water (12–17).

Previous work covered evaluating the efficiency of the application of ACFs in the removal of phenol from water. For an efficient adsorption process of ACFs in practical application, the fundamental kinetics of the adsorption process and the adsorption equilibrium should be considered in advance. Thus, one of the objectives of the present study is to research the adsorption equilibrium and adsorption kinetics in ACF fixed beds for the removal of phenol from water by experiments and theoretical methods.

A key to the economic operation process of adsorption is the ability to regenerate and reuse adsorbents because of the high initial cost of these adsorbents. The common techniques for desorption of phenol from adsorbents are thermal regeneration (18,19), chemical regeneration (20,21), and ultrasound regeneration (22). Because phenol is a weak acid, an increase in pH of phenol aqueous solution enhances the formation of phenate species ($C_6H_5O^-$), which cannot be adsorbed easily by adsorbents. So the second objective of our research is to apply the chemical methods for the regeneration of spent ACFs; the regenerability for spent ACF fixed bed is evaluated.

## MODELING OF ACTIVATED CARBON FIBER FIXED-BED ADSORBERS

Here we consider an isothermal bed packed with ACFs. The length-to-diameter ratio of ACF is so large that we can assume ACF to be a cylinder of infinite length. The bed was subjected to axial (longitudinal) dispersion, external film diffusion, and intraparticle (i.e., intrafiber) diffusion of the adsorbing species. It is assumed that the adsorption isotherm is of Langmuir type:

$$q = \frac{q_m Kc}{1 + Kc} \tag{1}$$

Then for a step concentration change (input), mass conservation of phenol in the fluid phase is

$$D_L \frac{\partial^2 C}{\partial Z^2} - u\frac{\partial C}{\partial Z} - \frac{\partial C}{\partial t} - \rho_p \frac{(1-\alpha)}{\alpha}\frac{\partial \overline{q}}{\partial t} = 0 \tag{2}$$

where

$$\overline{q} = \frac{2}{R^2}\int_0^R q(r, Z, t)\, rdr \tag{3}$$

The initial and boundary conditions for the ACF fixed bed are

$$D_L \left(\frac{\partial C}{\partial Z}\right)_{Z=0^-} = u[(C)_{Z=0^-} - C_0] \tag{4}$$

$$\left(\frac{\partial C}{\partial Z}\right)_{Z=L} = 0 \tag{5}$$

$$C(Z{,}0) = 0 \tag{6}$$

Mass conservation of phenol in the ACFs is

$$\varepsilon_p \frac{\partial C}{\partial t} + \rho_p \frac{\partial q}{\partial t} = D_p \frac{1}{r}\frac{\partial}{\partial r}\left(r\frac{\partial c}{\partial r}\right) \tag{7}$$

The initial and boundary conditions for Eq. (7) are

$$\left(\frac{\partial c}{\partial r}\right)_{r=0} = 0, \qquad \left(\frac{\partial q}{\partial r}\right)_{r=0} = 0 \tag{8}$$

$$D_p \left(\frac{\partial c}{\partial r}\right)_{r=R} = k_f[C - (c)_{r=R}] \tag{9}$$

$$c(r,Z,0) = 0 \quad (10)$$

$$q(r,Z,0) = 0 \quad (11)$$

Equations (2)–(11) are solved by an orthogonal collocation method, which transforms the actual system of partial differential Eqs. (2) and (7) into a system of ordinary differential equations of initial value type. In this paper, 8 radial collocation points for ACF and 11 axial collocation points for the fixed bed were selected, respectively. By applying the orthogonal collocation method to the mass conservation Eq. (7) in the ACF and to the mass conservation Eq. (2) in the fluid phase, $11 \times 8$ ordinary differential equations were obtained. These equations were integrated in the time domain using Gear's stiff variable step integration routine.

## MATERIALS AND EXPERIMENTAL METHODS

The felt viscose-based ACFs used in the experiments were provided by Anshan ACF plant, China. The diameter of single ACF is about 16 μm (measured by an optical microscope), density 812 kg/m$^3$, and porosity of ACFs 0.59. The $N_2$-BET surface area and the pore volume, which are measured by ASAP2400 are 902 m$^2$/g and 0.46 mL/g, respectively, in which the surface area and the pore volume of micropores (the diameter of pores less than 1.7 nm) are 862 m$^2$/g and 0.41 mL/g, respectively. The total acidic and basic functional groups are 0.2532 mmol/g and 0.3972 mmol/g, respectively (17).

The ACFs were boiled, washed three times in distilled water, and dried at 110°C for 24 h before use.

The phenol aqueous solution was prepared using reagent grade phenol. Adsorption of phenol onto ACFs is strongly dependent on pH of the solution. The pH value of the water being saturated by $CO_2$ is about 5.7, therefore, for our experiments, we adjusted the initial pH = 5.7 with 0.01 N NaOH and 0.01 N HCl.

### Measurement of Adsorption Isotherm and Breakthrough Curves

The air in the pores of ACFs (mass $W_A$) was replaced with distilled water under vacuum at 60°C. Several pieces of felt ACFs with the same mass (width 4 cm and adjustable length to keep the unity of the density of the packing bed) were rolled up as a cylinder and placed into a 300-mm-long acrylic column (the packing length of ACFs being $L$ and its inner diameter $d$). The column was filled with water in advance. Glass fibers and beads were placed at both ends of the ACF test section, used as the column support medium and distributor. The glass fibers and beads were immersed in an acid solution overnight and washed by distilled water before use.

Experiments were conducted at a temperature of 25°C. The phenol aqueous solution flows from a high level tank into the ACF column through a preheater. Columns were operated in the up flow mode. An overflow pipe controls the surface level of the phenol aqueous solution in the column to keep the rate in the column constant. A glass valve at the outlet of the column adjusts the fluid flow, $Q$. The concentrations of phenol in effluent solution were analyzed by UV751-G spectrophotometer at 288-nm wave length with the detection limit of 1.0 mg/L.

The method of measuring the isotherm data was as follows. A 400-mL flask was filled with 250 mL of known concentration of phenol solution, a magnetic stirrer, and a known mass of ACFs were added to the flask. The aqueous phenol solution in the flask was then continuously stirred. After 30 h (sufficient to attain the equilibrium state, as shown in the Appendix), the phenol concentration was determined; the adsorbed amount was derived from the mass balance.

### Regeneration of Saturated ACF Fixed Beds

The regeneration was first conducted in a batch adsorber to select the potential regenerants from 1, 2.5, and 5% NaOH aqueous solution at 25°C and 40°C, and ethanol at 25°C. The results showed that the efficiency of regeneration is up to 90% for both 25°C ethanol and 40°C 5% NaOH solution. By comparing the efficiency and the amount of regenerant needed in the regeneration, we selected 25°C ethanol and 40°C 5% NaOH solution as regenerants for further research in a fixed bed adsorber.

When the ACF fixed bed reaches the saturation with phenol, regeneration is carried out. The regenerant (650 mL of 5% NaOH solution or 200 mL of ethanol) is introduced into the fixed bed from a high level tank. The spent ACFs were immersed with the regenerant for 4 h by controlling the effluent rate of the regenerant. Preheater is used to control the temperature at 40°C for NaOH solution and at 25°C for ethanol. After regeneration, wash the fixed bed with distilled water or dilution HCl solution until pH = 5.7, then begin the next adsorption operation.

## RESULTS AND DISCUSSION

### Adsorption Isotherm

The adsorption equilibrium data for phenol on ACFs in aqueous solution was obtained from both batch experiments (open circle as shown in Fig. 1) and fixed bed experiments (solid circle as shown in Fig. 1) at 25°C for initial pH = 5.7. In the range of phenol concentrations from 0 to 0.8 kg/m$^3$, equilibrium data can be fitted by a Langmuir-type equation, i.e., Eq. (1), as shown in Fig. 1 (solid

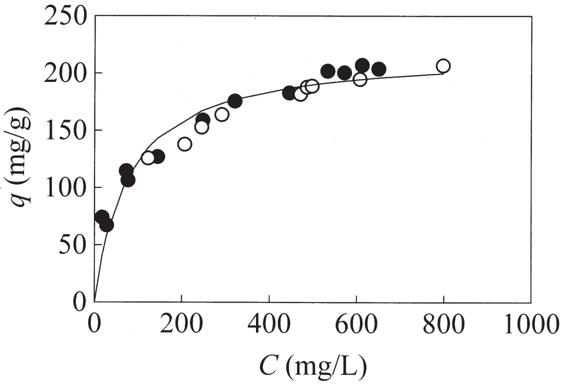

***Figure 1.*** Adsorption isotherm of phenol onto ACFs in aqueous solution (25°C, initial pH = 5.7). ——, Langmuir; ○, experiment by batch adsorber; ●, experiment by fixed bed adsorber.

line), in which the parameters are $K = 10.36$ m$^3$/kg and $q_m = 0.232$ kg/kg, respectively. The least squares method was used to fit the isothermal data and determine the Langmuir parameters, the mean error is about 2.3%.

The influence of pH on the adsorption capacity of ACFs is shown in Fig. 2a. It is evident that the effect of pH is negligible when pH $\leq$ 8.0, and a rapid decrease in the adsorption capacity of ACFs is found with an increase of pH when pH $>$ 8.0.

Phenol is a weak acid, an increase in pH enhances the formation of phenate species ($C_6H_5O^-$), which is not retained by ACFs (1). In fact the reaction taking place is

$$C_6H_5OH + OH^- \overset{K_{eq}}{\longleftrightarrow} C_6H_5O^- + H_2O$$

with reaction equilibrium constant

$$K_{eq} = [C_6H_5O^-]/([C_6H_5OH][OH^-]).$$

Assuming that $C_T$ is the molar concentration of phenol plus phenate in the solution, we have

$$C_T = [C_6H_5OH]\,(1 + K_{eq}[OH^-]) = [C_6H_5OH]\,(1 + K_{eq}10^{\mathrm{pH}-14}) \tag{12}$$

that is

$$\frac{[C_6H_5OH]}{C_T} = \frac{1}{1 + K_{eq}10^{\mathrm{pH}-14}} \tag{13}$$

and

$$\frac{[C_6H_5O^-]}{C_T} = 1 - \frac{1}{1 + K_{eq}10^{\mathrm{pH}-14}} \tag{14}$$

The effect of pH on the relative contributions of phenol speciation of $C_6H_5OH$ and $C_6H_5O^-$ is shown in Fig. 2b presuming that $K_{eq} = 1.3 \times 10^4$ L/mol for 20°C (1). It is evident that the concentration of phenol $[C_6H_5OH]$ decreases with increasing pH when pH $> 8.0$, which results in the decrease of the adsorbed amount as shown in Fig. 2a.

The pH value in the phenol aqueous solution should be controlled under acid condition for adsorption of phenol onto ACFs and under strong base condition for the regeneration of ACFs saturated with phenol.

## Breakthrough Behavior in ACF Fixed Bed

Experiments are carried out to measure the breakthrough curves in ACF fixed bed at various operating conditions, as shown in Fig. 3. The experimental

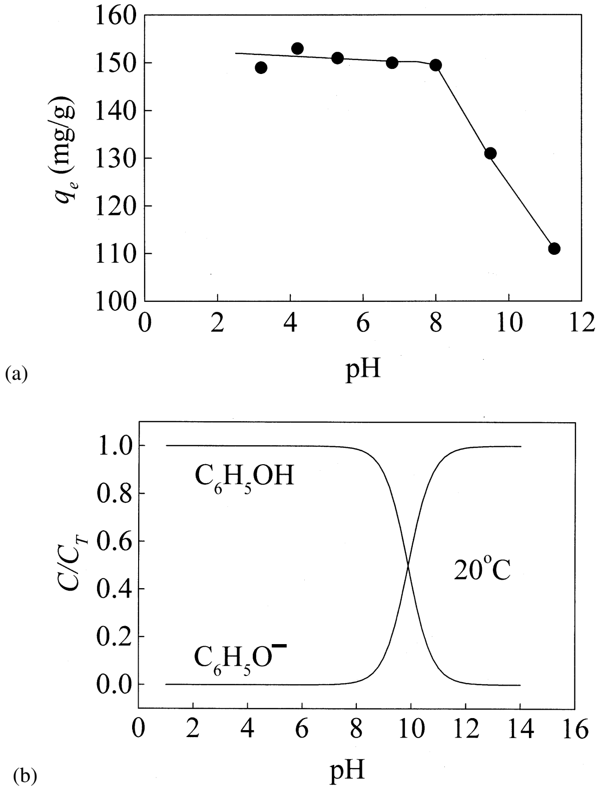

***Figure 2.*** (a) Effect of pH on the equilibrium adsorbed amount of phenol onto ACFs at 25°C, $C_0 = 0.897$ kg/m$^3$, $V_L = 100$ mL, and $W_A = 0.5$ g. (b) Effect of pH on the concentration distributions of phenol and phenate calculated by Eqs. (13) and (14).

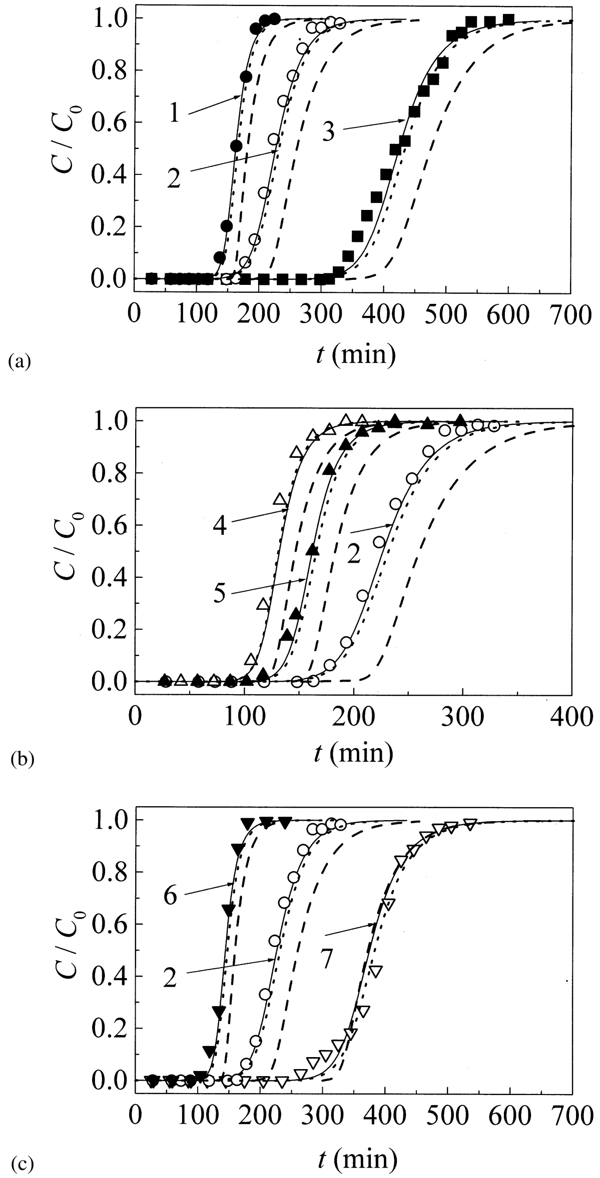

***Figure 3.*** (a) Effect of initial concentrations on breakthrough curves in ACF fixed bed. For the experimental conditions, see Table 1. (b) Effect of bed length on breakthrough curves in ACF fixed bed. For the experimental conditions, see Table 1. (c) Effect of fluid flow rate on breakthrough curves in ACF fixed bed. For the experimental conditions, see Table 1. Solid lines, Eqs. (1)–(11); dotted lines, Eqs. (19) and (20); dashed lines, Eq. (21).

***Table 1.*** Characteristics of ACF Fixed Bed, Experimental Conditions and Evaluated Model Parameters

| No. | $d$ mm | L mm | $W_A$ $g$ | $C_0$ g/m$^3$ | $Q$ l/h | α | $D_p \times 10^{10}$ m$^2$/s | $k_f \times 10^4$ m/s | $D_L \times 10^6$ m$^2$/s | ε |
|---|---|---|---|---|---|---|---|---|---|---|
| 1 | 19 | 192 | 7.64 | 797.6 | 0.72 | 0.824 | 4.12 | 1.81 | 6.5 (6.5[a], 18[b]) | 0.007 |
| 2 | 19 | 178 | 6.70 | 485.5 | 0.69 | 0.833 | 4.12 | 1.75 | 5.5 (5.5[a], 20[b]) | 0.014 |
| 3 | 19 | 188 | 8.04 | 244.9 | 0.75 | 0.810 | 4.12 | 1.87 | 2.5 (2.5[a], 15[b]) | 0.012 |
| 4 | 19 | 92 | 4.04 | 470.2 | 0.75 | 0.805 | 4.12 | 1.89 | 2.5 (2.5[a], 10[b]) | 0.013 |
| 5 | 19 | 141 | 5.63 | 485.5 | 0.81 | 0.823 | 4.12 | 1.88 | 4.0 (4.0[a], 15[b]) | 0.014 |
| 6 | 19 | 184 | 7.03 | 493.7 | 1.13 | 0.830 | 4.12 | 2.63 | 6.5 (6.5[a], 22[b]) | 0.011 |
| 7 | 19 | 181 | 6.71 | 505.0 | 0.456 | 0.836 | 4.12 | 1.52 | 2.5 (2.5[a], 10[b]) | 0.016 |

[a] Evaluated by the simpler model, i.e., Eqs. (19) and (20) (Fig. 3).

[b] Evaluated by the constant pattern profiles solution, i.e., Eq. (21) (Fig. 3).

conditions are summarized in Table 1. It is evident that the breakthrough curves and breakthrough time are strongly dependent on these experimental conditions, such as feed concentration (Fig. 3a), bed length (Fig. 3b), and fluid flow rate (Fig. 3c). The cases of higher feed concentration, higher flow rate or shorter bed length would make the ACF fixed bed breakthrough early.

By mathematical analysis, it will be found that the breakthrough curves from a packed bed can be predicted based on both the adsorption isotherm relation and the mass transfer parameters during the adsorption process. The mass transfer parameters include the external fluid-to-particle mass transfer coefficient, $k_f$, the intraparticle diffusivity, $D_p$, and the axial dispersion coefficient, $D_L$.

The intraparticle diffusivity, $D_p$, is not dependent on the form of adsorber, we evaluated $D_p$ in a batch tank at 25°C for initial pH = 5.7. The phenol concentration decay curves obtained experimentally were analyzed by the pore diffusion model (as shown in the Appendix) and it was found that, in the range of concentrations between 0 and 0.8 kg/m$^3$, the pore diffusion model fits the results well. The intraparticle diffusivity was evaluated to be about $4.12 \times 10^{-10}$ m$^2$/s.

The correlation of Wilson and Geankoplis (23) is adopted to evaluate the fluid-particle mass transfer coefficient, $k_f$:

$$\mathrm{Sh} = \left(\frac{1.09}{\alpha}\right)\mathrm{Sc}^{1/3}\mathrm{Re}^{1/3} \quad \text{for } 0.0015 < \mathrm{Re} < 55 \tag{15}$$

where Sherwood number $\mathrm{Sh} = 2k_f\ R/D_v$, Schmidt number $\mathrm{Sc} = \mu_w/(\rho_w D_v)$, Reynolds number $\mathrm{Re} = 2R\rho_w u/\mu_w$, in which the molecular diffusion coefficient $D_v$ of phenol in aqueous solution is obtained from the Wilke equation (23):

$$D_v = 7.4 \times 10^{-12}(\varphi M_f)^{1/2}\frac{T}{\mu_f V_A^{0.6}}\ (\mathrm{m}^2/\mathrm{s}) \tag{16}$$

in which association parameter $\varphi = 2.6$, molecular weight of water $M_f = 18.02$, absolute temperature $T = 298.15$ K, viscosity of water $\mu_f = 0.8937$ cP, and mole volume of adsorbate at normal boiling point $V_A = 118.4$ cm$^3$/mol.

Substituting these values into Eq. (16), $D_v = 9.6 \times 10^{-10}$ m$^2$/s.

The evaluated values of $k_f$ based on the above equation for our experimental conditions are listed in Table 1.

By comparison of the predicted breakthrough curves with the experimental data, the axial dispersion coefficient can be evaluated. The fitting is examined in terms of the root-mean-square error between $C_{\text{exp}}(t)$ and $C_{\text{calc}}(t)$:

$$\varepsilon = \frac{1}{C_0}\sqrt{\frac{1}{M}\sum_{m=1}^{M}[C_{\text{exp}}(t_m) - C_{\text{calc}}(t_m)]^2} \tag{17}$$

Figure 3 shows the best-fit curves calculated by the orthogonal collocation method (solid lines). The experimental conditions and evaluated parameters for Fig. 3 are summarized in Table 1.

With numerical inspection, we found that if $D_p \geq 1.0 \times 10^{-10}$ m$^2$/s, these curves do not change with increasing $D_p$. Because the values of $D_p$ evaluated by the batch experiments were about $4.12 \times 10^{-10}$ m$^2$/s, the intraparticle mass transfer resistance is not the rate-controlling step for the ACF fixed bed. It is also interesting that $k_f$ almost has not affected the breakthrough curves, the fluid-to-fiber mass transfer resistance could be neglected for the ACF fixed bed experimental system. This is coincident with the theoretical analysis (24,25), i.e., if the bed length parameter $(LD_pC_0)/(uR^2\rho_p q(C_0)) > 1$ (for our experimental conditions it is in the range of 1.5–7.0), the fluid-to-fiber mass transfer resistance is also not the mass transfer rate-controlling step. Therefore, it should be obvious that for the present experiments (i.e., at lower Re), the main factor affecting the breakthrough curves is the axial dispersion coefficient, $D_L$. Suzuki and coworkers (14) have reached the same conclusion.

For the present experimental conditions, $D_L$ was evaluated to be about $2.5\text{–}6.5 \times 10^{-6}$ m$^2$/s. Usually $D_L$ is considered to consist of contributions of the molecular diffusion and the dispersion caused by fluid flow:

$$D_L = D_{L,molecular} + D_{L,flow} \tag{18}$$

Generally, the contribution of molecular diffusion becomes dominant in the range of Sc Re < 10. However, in a packed bed of particles smaller than 2 mm, attention should be paid to a high contribution of dispersion due to fluid flow (23). This is likely to be due to the channeling of flow induced by the local irregularity of packing conditions. For ACF packed bed, due to ACFs being very narrow, the local irregularity of packing conditions is more serious. Under this condition, ignoring the effect of $D_L$ on the breakthrough curves will cause great error.

Suzuki (14) obtained the diagram of Peclet number $Pe_F$ and the density of the fixed bed packed with ACFs, $\rho_B$, where the definitions of $Pe_F$ and $\rho_B$ are $Pe_F = 2Ru/D_L$ and $\rho_B = W_A/(\pi d^2L/4)$, in which $u = Q/(\pi d^2\alpha/4)$.

Marcel Dekker, Inc.
270 Madison Avenue, New York, New York 10016

For our experiments, the change of $\rho_B$ is from 0.131 g/mL (for run 7) to 0.155 g/mL (for run 2), the corresponding values of $Pe_F$ are $1.40 \times 10^{-3}$ and $1.25 \times 10^{-3}$ based on the diagram of Suzuki (14). The values of $D_L$ are then evaluated to be $6.8 \times 10^{-6}$ m$^2$/s and $10.4 \times 10^{-6}$ m$^2$/s, respectively, which are bigger than those obtained from our experiments as listed in Table 1. Owing to the importance of the axial dispersion and lack of the correlation of $D_L$, it would be desirable to attempt to measure $D_L$ independently, and find the general correlation of $D_L$ with the operating conditions and the properties of the adsorption system, this would be of key importance for design purposes.

We have asserted that for low Reynolds numbers used in this research neither external nor internal mass transfer is rate limiting. If the axial dispersion is acting alone, Eqs. (1)–(11) for fixed bed adsorption can be simplified as follows:

$$D_L \frac{\partial^2 C}{\partial Z^2} - u\frac{\partial C}{\partial Z} - \frac{\partial C}{\partial t} - \rho_p \frac{(1-\alpha)}{\alpha}\frac{\partial \overline{q}}{\partial t} = 0 \tag{19}$$

$$\overline{q} = \frac{q_m KC}{1 + KC} \tag{20}$$

with boundary conditions $(C)_{Z=0} = C_0$, $(\partial C/\partial Z)_{Z=L} = 0$, and initial conditions $C = 0$ and $\overline{q} = 0$ at $t = 0$.

Equations (19) and (20) were solved by the orthogonal collocation method as mentioned above.

Furthermore, if ignoring the term of $\partial C/\partial t$ in Eq. (19), the following analytical solution can be obtained based on the constant pattern profiles assumption (17):

$$Pe_B\left(1 - \frac{\tau}{\delta}\right) = \frac{1}{1-\lambda}\left[\ln\left(1 - \frac{C}{C_0}\right) - \lambda \ln\left(\frac{C}{C_0}\right)\right] \tag{21}$$

where Peclet number $Pe_B = uL/D_L$, dimensionless time $\tau = tu/L$, distribution ratio $\delta = \rho_p q(C_0)(1-\alpha)/(\alpha C_0)$, and equilibrium constant $\lambda = 1/(1 + KC_0)$.

The dotted and dashed lines in Fig. 3, respectively, correspond to the best-fit results calculated by the simpler model, i.e., Eqs. (19) and (20), and the constant pattern profiles solution, i.e., Eq. (21). The dotted lines are close to the solid lines and the evaluated values of $Pe_B$ are the same. This means the simpler model, based solely on a liquid phase mass balance and incorporating local equilibrium with axial dispersion, provides a good description of the process. But the constant pattern profiles solution (dashed lines) fails to represent the orthogonal collocation method (solid lines) in part due to the lower values of $Pe_B$ and $\delta$ for the present experimental conditions.

## Regeneration of Saturated ACF Fixed Beds

The regeneration of ACFs saturated with phenol in fixed bed is achieved by using ethanol and hot sodium hydroxide, respectively. Figure 4 shows the com-

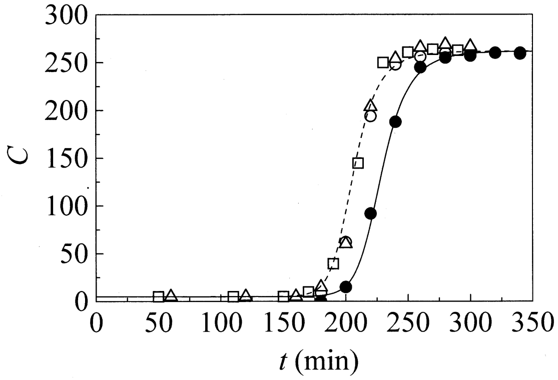

***Figure 4.*** Comparison of breakthrough curves of regenerated ACF fixed bed with that of fresh ACF fixed bed at $L$ = 103 mm, $W_A$ = 4.371 g, $Q$ = 11.75 mL/min, $C_0$ = 261 mg/L, and $\alpha$ = 0.812. Lines, simulating $D_p = 4.12 \times 10^{-10}$ m$^2$/s, $D_L = 9.2 \times 10^{-6}$ m$^2$/s, m$^2$/s, and $k_f = 1.86 \times 10^{-4}$ m/s; ●, fresh ACF; ○, first regeneration with 5% NaOH at 40°C; □, second regeneration with 5% NaOH at 40°C; □, third regeneration with ethanol at 25°C.

parison of the breakthrough curves in fresh ACF fixed bed and in regenerated ACF fixed bed at almost the same adsorption experimental conditions of $L$ = 103 mm, $W_A$ = 4.371 g, $Q$ = 11.75 mL/min, $C_0$ = 261 mg/L, and $\alpha$ = 0.812 for the removal of phenol from aqueous solution. The regenerant of 5% NaOH solution at 40°C is used for the first regeneration of ACF fixed bed, for the second and the third regeneration, the regenerants are 5% NaOH solution at 40°C and ethanol at 25°C, respectively. The adsorption capacity of regenerated ACFs is lower than that of fresh ACFs, which leads to the early breakthrough for regenerated ACF fixed bed, but the efficiency of regeneration is almost kept up to 90% for multiple regenerated ACF fixed bed.

The breakthrough curves for regeneration processes were simulated by Eqs. (2)–(11) (dashed lines as shown in Fig. 4) with $D_p = 4.12 \times 10^{-10}$ m$^2$/s, $D_L = 9.2 \times 10^{-6}$ m$^2$/s, $k_f = 1.86 \times 10^{-4}$ m/s, and with the following modified adsorption isotherm:

$$q = \eta \frac{q_m K c}{1 + Kc} \tag{22}$$

in which $\eta$ is the efficiency of regeneration.

As shown in Fig. 4, the simulating results fit the experimental data well.

## CONCLUSIONS

Activated carbon fibers (ACFs) are more effective adsorbents for the adsorption of phenol if pH in aqueous solution is controlled under acid condition.

Marcel Dekker, Inc.
270 Madison Avenue, New York, New York 10016

The adsorption capacity of ACFs is favorable and the adsorption isothermal data can be represented by a Langmuir equation for the range of phenol concentrations from 0 to 0.8 kg/m$^3$. The regeneration of ACFs saturated with phenol in fixed bed can be achieved by using ethanol or hot sodium hydroxide solution, respectively, for many times with 90% efficiency of regeneration.

The mathematical model was developed for ACF fixed bed and was used to predict the breakthrough curves. The results showed that the effect of the axial dispersion on breakthrough curves is apparent, and it cannot be negligible at a lower Reynolds number for ACF fixed bed. The intraparticle and external mass transfer resistances are not the rate-controlling steps, the reason of which is attributable to the short diffusion path for adsorbate in ACFs.

A simpler model, based solely on a liquid phase mass balance and incorporating local equilibrium with axial dispersion, provides a good description of the process. But the constant pattern profiles solution fails to represent the orthogonal collocation method in part due to the lower values of Peclet number $Pe_B$ and distribution ratio δ for the present experimental conditions.

## APPENDIX

For the batch adsorber, the mathematical model with pore diffusion mode is

$$\varepsilon_p \frac{\partial c}{\partial t} + \rho_p \frac{\partial q}{\partial t} = D_p \frac{1}{r} \frac{\partial}{\partial r}\left( r \frac{\partial c}{\partial r} \right) \tag{1A}$$

$$V_L \frac{dC}{dt} + \frac{2W_A}{\rho_p R} k_f \left[ C - (c)_{r=R} \right] = 0 \tag{1B}$$

$$D_p \left( \frac{\partial c}{\partial r} \right)_{r=R} = k_f [C - (c)_{r=R}] \tag{1C}$$

$$\left( \frac{\partial c}{\partial r} \right)_{r=0} = 0, \qquad \left( \frac{\partial q}{\partial r} \right)_{r=0} = 0 \tag{1D}$$

$$t = 0, \qquad C = C_0, \qquad c = 0, \qquad q = 0 \tag{1E}$$

where $V_L$ is the volume of the fluid in the batch adsorber.

Figure 1A shows the comparison of the measured concentration time data with the best-fit curve predicted by the pore diffusion model at 25°C for initial pH = 5.7 under the conditions of $C_0 = 0.8$ kg/m$^3$, $V_L = 250$ mL, and $W_A = 0.825$ g. From which, the intraparticle diffusivity for pore diffusion mode was evaluated to be $D_p = 4.12 \times 10^{-10}$ m$^2$/s. The fitting error is $\varepsilon = 0.015$.

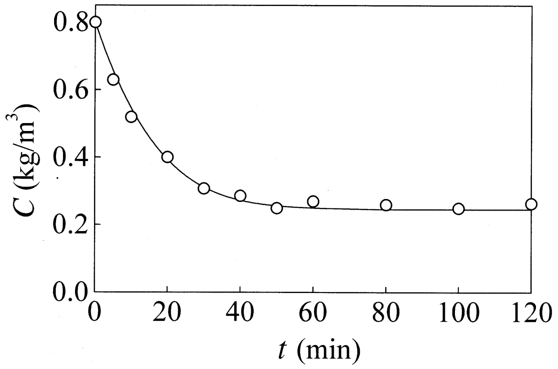

***Figure 1A.*** Comparison of the measured concentration-time data with the best-fit curve predicted by the pore diffusion model in a batch adsorber at 25°C for initial pH = 5.7 at $C_0 = 0.8$ kg/m$^3$, $V_L = 250$ mL, and $W_A = 0.825$ g.

## NOMENCLATURE

| | |
|---|---|
| $c$ | concentration in particles (fibers) (kg/m$^3$) |
| $C$ | concentration in fluid (kg/m$^3$) |
| $C_0$ | inlet concentration in fluid (kg/m$^3$) |
| $C_T$ | molar concentration of phenol plus phenate in the solution (mol/m$^3$) |
| $d$ | diameter of packing ACF in the column (m) |
| $D_L$ | axial dispersion coefficient based on adsorber length (m$^2$/s) |
| $D_p$ | diffusivity in pores of adsorbent (m$^2$/s) |
| $K$ | adsorption equilibrium constant defined by Eq. (1) (m$^3$/kg) |
| $K_{\mathrm{eq}}$ | reaction equilibrium constant (m$^3$/mol) |
| $k_f$ | fluid-to-particle mass transfer coefficient (m/s) |
| $L$ | packing length of ACFs in the column (m) |
| $Pe_F$ | Peclet number based on a single ACF length |
| $Pe_B$ | Peclet number based on adsorber length |
| $q$ | internal concentration in particles (kg/kg) |
| $Q$ | fluid flow (m$^3$/s) |
| $q_m$ | adsorption equilibrium constant defined by Eq. (1) (kg/kg) |
| $r$ | radial distance from center of particle (m) |
| $R$ | radius of fiber (m) |
| $t$ | time (s) |
| $u$ | average velocity in the interparticle space in the column (m/s) |
| $W_A$ | mass of ACFs (kg) |
| $Z$ | axial distance from column entrance (m) |

## Greek Letters

| | |
|---|---|
| $\alpha$ | bed porosity ($m^3/m^3$) |
| $\varepsilon$ | root-mean-square error defined by Eq. (17) |
| $\varepsilon_p$ | adsorbent porosity ($m^3/m^3$) |
| $\mu_w$ | dynamic viscosity of water ($Pa \cdot s$) |
| $\rho_B$ | density of the fixed bed ($kg/m^3$) |
| $\rho_p$ | density of porous particle ($kg/m^3$) |
| $\rho_w$ | density of water ($kg/m^3$) |

## ACKNOWLEDGMENTS

We thank two anonymous reviewers for helpful comments.

## REFERENCES

1. Costa, C.; Rodrigues, A. Design of Cyclic Fixed-Bed Adsorption Processes. AIChE J. **1985**, *31*, 1645–1665.
2. Wang, R.C.; Kuo, C.C.; Shyu, C.C. Adsorption of Phenols onto Granular Activated Carbon in a Liquid-Solid Fluidized Bed. J. Chem. Tech. Biotechnol. **1997**, *68*, 187–194.
3. Allsop, P.J.; Chisti, Y.; Young, M.M.; Sullivan, G.R. Dynamics of phenol degradation by pseudomonas putida. Biotechnol. Bioeng. **1993**, *41*, 572–580.
4. Wu, Y.; Taylor, K.E.; Biswas, N.; Bewtra, J.K. Kinetic Model for Removal of Phenol by Horseradish Peroxidase with PEG. J. Environ. Eng. **1999**, *125*, 451–458.
5. Buchanan, I.D.; Nicell, J.A. A Simplified Model of Peroxidase-Catalyzed Phenol Removal from Aqueous Solution. J. Chem. Technol. Biotechnol. **1999**, *74*, 669–674.
6. Calleja, G.; Serna, J.; Rodriguez, J. Kinetics of Adsorption of Phenolic Compounds from Wastewater onto Activated Carbon. Carbon **1993**, *31*, 691–697.
7. Wang, R.C.; Yang, J.J. Competitive Adsorption of Bisolute Phenols onto Granular Activated Carbon. J. Chin. Inst. Chem. Engrs. **1997**, *28*, 185–195.
8. Teng, H.; Hsieh, C.T. Liquid-Phase Adsorption of Phenol by Activated Carbons Prepared from Bituminous Coals with Different Oxygen Contents. J. Chem. Tech. Biotechnol. **1999**, *74*, 123–130.

9. Kwon, S.C.; Song, D.I.; Jeon, Y.W. Adsorption of Phenol and Nitrophenol Isomers onto Montamorillonite Modified with Hexadecyltrimethylannonium Cation. Sep. Sci. Technol. **1998,** *33*, 1981–1998.
10. Furuya, E.; Takeuchi, Y.; Noll, K.E. Intraparticle Diffusion of Phenols within Bidispersed Macroreticular Resin Particles. J. Chem. Eng. Japan, **1989**, *22*, 670–676.
11. Goto, S.; Goto, M.; Uchiyama, S. Adsorption Equilibria of Phenol on Anion Exchange Resins in Aqueous Solution. J. Chem. Eng. Japan **1984**, *17*, 204–205.
12. Nitta, T.; Suzuki, T.; Katayama, T. Gas-phase adsorption equilibria for acetone, diethyl ether, methanol, and water on activated carbon fiber. J. Chem. Eng. Japan. **1991**, *24*, 160–165.
13. Brasquet, C.; Cloirec, P.L. Adsorption onto activated carbon fibers: application to water and air treatments. Carbon **1997**, *35*, 1370–1313.
14. Suzuki, M. Activated Carbon Fiber: Fundamentals and Applications. Carbon **1994**, *32*, 577–586.
15. Xiu, G.H.; Li, P.; Jin, G. Adsorption Characteristics of Activated Carbon Fiber in a Batch Tank. J. Chem. Industry & Eng. (China) **1995**, *46*, 571–575.
16. Li, P.; Xiu, G.H.; Jin, G. Prediction of Breakthrough Curves in Fixed-Bed Adsorbers of Activated Carbon Fiber. (2) Experiments and Models Test. J. Chem. Industry & Eng. (China) **1997**, *48*, 277–283.
17. Xiu, G.H.; Li, P. Prediction of Breakthrough Curves for Adsorption of Lead (II) on Activated Carbon Fibers in a Fixed-Bed. Carbon **2000**, *38*, 975–981.
18. Suzuki, M.; Misic, D.M.; Koyama, O.; Kawazoe, K. Study of thermal regeneration of spent activated carbon: thermogravimetric measurement of various single component organics loaded on activated carbon. Chem. Eng. Sci. **1978**, *33*, 271–279.
19. Moreno-castilla, C.; Rivera-Utrilla, J.; Joly, J.P.; Lopez-Ramon, M.V.; Ferro-Garcia, M.A.; Carrasco-Marin, F. Thermal regeneration of activated carbon exhausted with different substituted phenols. Carbon **1995**, *33*, 1417–1423.
20. Grant, T.M.; King, C.J. Mechanism of Irreversible Adsorption of Phenolic Compounds by Activated Carbon. Ind. Eng. Chem. Res. **1990**, *29*, 264–271.
21. Kilduff, J.E.; King, C.J. Effect of Carbon Adsorbent Surface Properties on the Uptake and Solvent Regeneration of Phenol. Ind. Eng. Chem. Res. **1997**, *36*, 1603–1613.
22. Rege, S.U.; Yang, R.T.; Cain, C.A. Desorption by Ultrasound: Phenol on Activated Carbon and Polymeric Resin. AIChE J. **1998**, *44*, 1519–1528.
23. Suzuki, M. *Adsorption Engineering*; Elsevier: Amsterdam, 1990.

24. Xiu, G.H. Modeling Breakthrough Curves in a Fixed Bed of Activated Carbon Fiber—Exact Solution and Parabolic Approximation. Chem. Eng. Sci. **1996**, *51*, 4039–4041.
25. Xiu, G.H.; Nitta, T.; Li, P.; Jin, G. Breakthrough Curves for Fixed-Bed Adsorbers: Quasi-Lognormal Distribution Approximation. AIChE J. **1997**, *43*, 979–985.

Received March 2000
Revised August 2000

Marcel Dekker, Inc.
270 Madison Avenue, New York, New York 10016

Downloaded At: 10:45 25 January 2011

# Request Permission or Order Reprints Instantly!

Interested in copying and sharing this article? In most cases, U.S. Copyright Law requires that you get permission from the article's rightsholder before using copyrighted content.

All information and materials found in this article, including but not limited to text, trademarks, patents, logos, graphics and images (the "Materials"), are the copyrighted works and other forms of intellectual property of Marcel Dekker, Inc., or its licensors. All rights not expressly granted are reserved.

Get permission to lawfully reproduce and distribute the Materials or order reprints quickly and painlessly. Simply click on the "Request Permission/Reprints Here" link below and follow the instructions. Visit the U.S. Copyright Office for information on Fair Use limitations of U.S. copyright law. Please refer to The Association of American Publishers' (AAP) website for guidelines on Fair Use in the Classroom.

The Materials are for your personal use only and cannot be reformatted, reposted, resold or distributed by electronic means or otherwise without permission from Marcel Dekker, Inc. Marcel Dekker, Inc. grants you the limited right to display the Materials only on your personal computer or personal wireless device, and to copy and download single copies of such Materials provided that any copyright, trademark or other notice appearing on such Materials is also retained by, displayed, copied or downloaded as part of the Materials and is not removed or obscured, and provided you do not edit, modify, alter or enhance the Materials. Please refer to our Website User Agreement for more details.

**Order now!**

Reprints of this article can also be ordered at

http://www.dekker.com/servlet/product/DOI/101081SS100105910